# Generalized formula for the stability and instability criteria of current-voltage characteristics measurements in the negative differential conductance region of a resonant tunneling diode

Chih Yuan Huang
*Department of Electronic Communication Engineering, National Kaohsiung Institute of Marine Technology, Kaohsiung 811, Taiwan, Republic of China*

James E. Morris
*Department of Electrical Engineering, State University of New York, Binghamton, New York 13902*

Yan Kuin Su[a)]
*Department of Electrical Engineering, National Cheng Kung University, Tainan 701, Taiwan, Republic of China*

(Received 19 November 1996; accepted for publication 8 May 1997)

A formula in terms of the equivalent circuit parameters of a resonant tunneling diode (RTD) and its loading for three different equivalent circuit models of RTD's is derived to describe the apparent change, occurring in the presence of unstable oscillation, in the negative differential conductance (NDC) region of dc current-voltage ($I$-$V$) characteristics measurements. The measured experimental $I$-$V$ data and the related parameters of RTD's from several fabricated devices are applied to the formula in terms of the stability and instability criteria to do the numerical verification. It has shown good agreement between the derived formula and the experimental $I$-$V$ data of RTD. Simulated program with integrated circuits emphases (SPICE) simulation shows the flattened and the broken sections, which represent the occurrence of the unstable oscillation, appearing in the NDC region of $I$-$V$ curve, which also validates the applicability of the derived formula. © *1997 American Institute of Physics.* [S0021-8979(97)00316-2]

## I. INTRODUCTION

There has been interest in the study of the current-voltage ($I$-$V$) characteristics of resonant-tunneling quantum well devices due to the fact that high frequency oscillator application arises from the gain provided by the negative differential conductance (NDC). Several recent studies[1–4] have focused on the effect of the circuit unstable oscillations for the measurement of $I$-$V$ characteristics of a resonant tunneling diode (RTD). When the RTD device is biased in the NDC region and the measuring circuit meets certain criteria, there has been a phenomenon of instability or characteristic "plateaulike," "chair-shaped," discontinuous structure which occurs in the NDC region instead of obtaining a stable, continuous dc $I$-$V$ curve tracing. This oscillation often appears as discontinuity in the measurement of dc $I$-$V$ characteristics, even if oscillating voltages do not appear at the voltmeter. It is, however, possible to predict some aspects of this unstable nature of the RTD circuit operating point (the intersection of the $I$-$V$ characteristics and the load line) and distinguish the threshold point between stable and unstable conditions by using an electrical circuit analytical approach. The circuit theories are applied to the RTD equivalent circuit of a typical measuring setup, which includes the oscillation factors such as inductance and capacitance in the device, and a loading to represent the measuring facility, to determine the criteria of this oscillation phenomenon. Two developed models,[5,6] differing from the conventional structures, which consists of a parasitic series resistance $R_S$ in series with the parallel combination of an intrinsic capacitance and an NDC element $R_D$, with an extra inductance added in each model to represent the time delay of current with respect to the applied voltage, are analyzed. A proposed model structure from mixing both prementioned models is also discussed so as to compare its stability and instability criteria to the others. In this article, we first dynamically analyze these three models with a proposed nonlinear element (i.e., $dv_j/di_j$) replacing those of the constant NDC element $R_D$. Second, several RTD devices fabricated in other laboratories will be adopted as RTD samples which are also being tested using the derived formulas of stability criteria to predict if the continuous (stable) or discontinuous (unstable oscillation) NDC region of $I$-$V$ characteristics of RTD will occur, to validate the applicability of the derived instability criteria. It has found that although the derived stability and instability criteria for the prementioned three models are somewhat different from each other due to the different structure of the equivalent circuit model, they have the same applicability to predict the unstable oscillation region in $I$-$V$ characteristics of RTD. At last, the derived formulas of the instability criteria for these three different models are verified by using the simulated program with integrated circuits emphases (SPICE) simulation to examine the validity of the derived results. In the simulation of the $I$-$V$ characteristics of RTD we have demonstrated for the first time the flattened and broken manners in the NDC region, which match the theoretical prediction that the unstable oscillation will occur in the NDC region if the parameters of the RTD device and circuit load meet the derived instability criteria.

[a)]Electronic mail: yksu@mail.ncku.edu.tw

 0021-8979/97/82(5)/2690/7/$10.00 

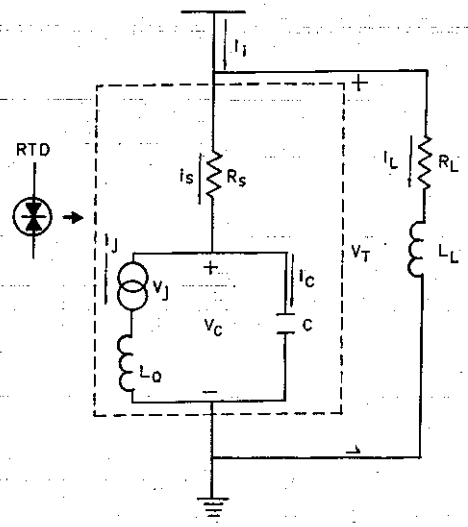


FIG. 1. Equivalent circuit model of the RTD from Gering *et al.*[5] model, and its loading, with the NDC element $R_D$ replaced by a nonlinear element $dv_j/di_j$.

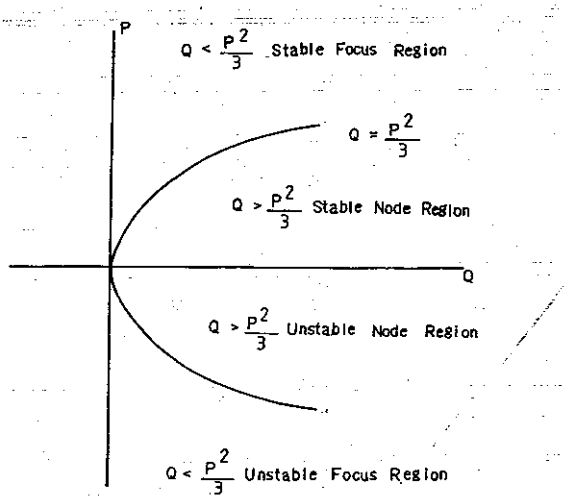


FIG. 2. Operating point behavior specified on $P$-$Q$ plane.

## II. THEORY

There exists many equivalent circuit models of RTD for different application purposes,[5–9] of which two notable inductive models are considered first in the following analyses. The third model is proposed from combining the above two models and is briefly discussed.

### A. Model (a)

Based on Gering *et al.*[5] model as shown in Fig. 1, the problem of the stable and unstable condition when biasing in the NDC region can be derived from the $i_s$–$v_j$ and $i_S$–$v_T$ relationships, and the large-signal behavior of the circuit is governed by

$$I_i = i_s + i_L, \tag{1a}$$

$$i_s = i_j + C\frac{dv_j}{dt}, \tag{1b}$$

$$(L_Q + L_L)\frac{di_s}{dt} = I_i R_L - i_s(R_L + R_S) - v_j, \tag{1c}$$

where $L_Q$ is the uncharacterized inductance and $L_L$ is the stray inductance. The behavior of a trajectory near the intersection of the load line and the characteristics of the $i_j$–$v_j$ plane, and the determination of the nature of the singularity can be solved from the above differential equations of Eq. (1). For the $i_s$–$v_j$ case, Eq. (1) becomes

$$\frac{di_s}{dt} = -\frac{R}{L}i_s - \frac{1}{L}v_j, \tag{2a}$$

$$\frac{dv_j}{dt} = \frac{1}{C}i_s - \frac{1}{R_D C}v_j, \tag{2b}$$

where $R = R_S + R_L$, $L = L_Q + L_L$, $R_D = dv_j/di_j$, $R_D$ is the negative differential resistance of RTD, and $R_D < 0$. There is a general theory by means of which the class of singularity may be found conveniently from the circuit parameters.[7] Thus we take Laplace transformation from Eq. (2), and it will be reduced to a canonical form as

$$\frac{dx}{dt} = S_1 x,$$

$$\frac{dy}{dt} = S_2 y.$$

The class of the singularity is related to the nature of $S_1$ and $S_2$, which are the two eigenvalues (two roots) of the quadratic eigen (characteristic) equation as $S^2 + PS + Q = 0$,[8] where

$$P = \frac{R}{L} + \frac{1}{R_D C},\quad Q = \frac{1}{LC}\left(1 + \frac{R}{R_D}\right).$$

When $P$ and $Q$ are used as rectangular coordinates as in Fig. 2, points representing singularities of different classes fall into the stable and unstable regions separated by the coordinate axes and the parabola $P^2 = 4Q$, as shown in Fig. 2. To solve the stability and instability conditions of the trajectory during curve tracing in the NDC region it requires $P > 0$, $Q > 0$, and $P < 0$, $Q > 0$, respectively. Thus, we can get the stability and instability criteria as shown in Eqs. (3a) and (3b), respectively,

$$\frac{L}{|R_D|C} < R < |R_D|, \tag{3a}$$

$$R < \frac{L}{|R_D|C},\quad R < |R_D|. \tag{3b}$$

For the more practical $i_S$–$v_T$ case (since we cannot directly measure the junction voltage $v_j$), Eq. (1) can be rearranged as

$$\frac{di_s}{dt} = -\frac{R_L}{L_L}i_s - \frac{1}{L_L}v_T, \tag{4a}$$

$$\frac{dv_T}{dt} = \frac{\alpha}{\beta}i_s - \frac{\gamma}{\delta}v_T, \tag{4b}$$

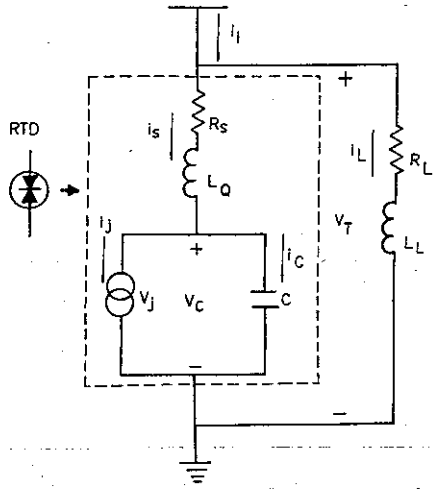


FIG. 3. Equivalent circuit model of the RTD from Brown *et al.* model, and its loading, with the NDC element $R_D$ replaced by a nonlinear element $dv_j/di_j$.

where

$$\alpha=L_L^2(R_D+R_S)-R_LL_L(L_Q+R_DR_SC)+R_L^2R_DL_QC,$$

$$\beta=\delta=R_DCL_LL,$$

and

$$\gamma=L_L^2+L_LL_Q+R_SR_DL_LC-R_DR_LL_QC;$$

similarly, the values of $P$ and $Q$ for Eq. (4) can be determined as

$$P=\frac{L+RR_DC}{LR_DC},\quad Q=\frac{R+R_D}{LR_DC}.$$

Applying the stable and unstable conditions of $P>0$, $Q>0$, and $P<0$, $Q>0$ again to Eq. (4), we obtain the same stability and instability criteria as Eq. (3).

### B. Model (b)

Using the same model as suggested from the experimental evidence by Brown *et al.*[6] except with the NDC element $R_D$ replaced by a nonlinear element $dv_j/di_j$, as shown in Fig. 3, we can write the circuit equations as follows:

$$L_L\frac{di_L}{dt}+i_LR_L=i_SR_S+v_C, \tag{5a}$$

$$I_i=i_S+i_L, \tag{5b}$$

$$i_S=i_j+C\frac{dv_c}{dt}, \tag{5c}$$

$$v_c=v_j+L_Q\frac{di_j}{dt}. \tag{5d}$$

By letting $I_i=0$, $R=R_L+R_S$, Eq. (5) can be manipulated and expressed in three-order differential equation form:

$$\frac{d^3i_S}{dt^3}+\left(\frac{R}{L_L}+\frac{R_D}{L_Q}\right)\frac{d^2i_S}{dt^2}+\left(\frac{RR_D}{L_QL_L}+\frac{1}{L_LC}+\frac{1}{L_QC}\right)\frac{di_S}{dt}+\frac{R+R_D}{L_QL_LC}i_s=0, \tag{6}$$

where $L_Q$ stands for the quantum well inductance and $L_L$ is the stray inductance. Taking Laplace transformation again from Eq. (6), the following cubic characteristic equation with three eigenvalues can determine the stability and instability criteria of the trajectory $S^3+PS^2+QS+T=0$, where

$$P=\frac{R}{L_L}+\frac{R_D}{L_Q},\quad Q=\frac{RR_D}{L_QL_L}+\frac{1}{L_QC}+\frac{1}{L_LC},\quad T=\frac{R+R_D}{L_QL_LC}. \tag{7}$$

*Case 1:* Assuming the measurement of RTD characteristics is in ideal condition, $L_L=0$ and $R_S=0$, then $R=R_L$ and Eq. (6) can reduce to second order form

$$\frac{d^2i_s}{dt^2}+\left(\frac{1}{R_LC}+\frac{R_D}{L_Q}\right)\frac{di_s}{dt}+\left(\frac{R_D}{R_L}+1\right)\frac{i_s}{L_QC}=0, \tag{8}$$

and from Eq. (8) we can obtain the values of $P$ and $Q$ as follows:

$$P=\frac{R_D}{L_Q}+\frac{1}{R_LC},\quad Q=\frac{1+\frac{R_D}{R_L}}{L_QC}. \tag{9}$$

Applying the stable condition of $P>0$, $Q>0$ and the unstable condition of $P<0$, $Q>0$ into Eq. (9), it yields the stability and instability criteria as shown in Eqs. (10a) and (10b), respectively,

$$|R_D|<R_L<\frac{L_Q}{|R_D|C}, \tag{10a}$$

$$R_L<\frac{L_Q}{|R_D|C},\quad R_L<|R_D|. \tag{10b}$$

Notice here that for the stability criteria, the inequality of Eq. (10a) is just opposite to Eq. (3a). It is found, however, that the instability criteria for both formulas, Eqs. (10b) and (3b), are basically the same, except the total inductance $L$ in Eq. (3b) is replaced by a quantum inductance $L_Q$. The formula derived in Eq. (3) from Gering *et al.*'s model does not tell which element ($L$ or $C$) will play the main character to cause the instability, but it exposes the fact that the smaller $RC$ time constant ($|R_D|C$) in the NDC region may result in oscillation when the ratio of the total amount of inductance in the circuit to $|R_D|C$ time constant is larger than $R$. Since the inductance $L_Q$ was not cleared from the published literature at the time, its cause is not as easily defined. Therefore we may attribute this uncharacterized inductance as part of the st ray inductance $L_L$ since they both are in the same loop.

Brown *et al.*[6] reported a new equivalent circuit model of RTD, and the addition of the "quantum well inductance" is well explained by the higher maximum oscillation frequency than predicted by the model of resistance and capacitance elements alone. The quantum well inductance and the undefined inductance in Gering's model both cause a time delay associated with the electrons being stored in the quantum

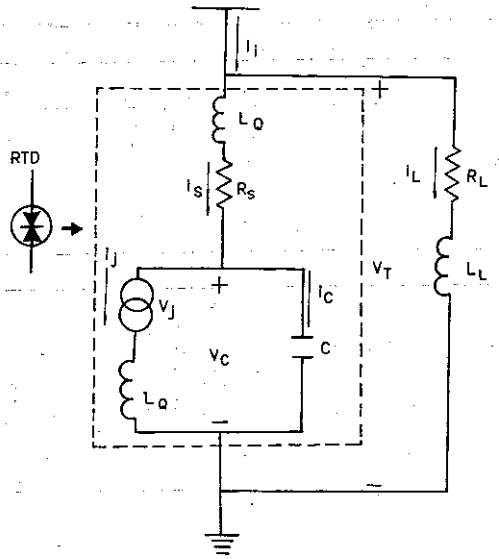


FIG. 4. A proposed equivalent circuit model of the RTD from mixing Figs. 1 and 2, and its loading, with the NDC element $R_D$ replaced by a nonlinear element $dv_j/di_j$.

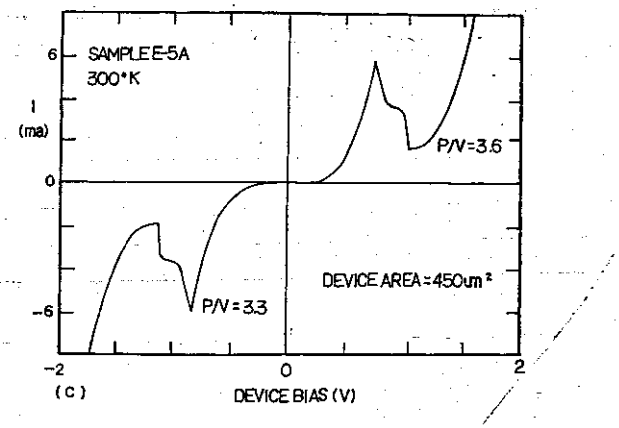


FIG. 5. Experimental $I$-$V$ characteristics of RTD sample 1 adopted from Huang *et al.* (Ref. 15).

well before tunneling out and produce a phase delay in the impedance of the RTD, and these similarities result in the same instability criteria as seen in Eqs. (3b) and (10b) regardless of the inductance position in the equivalent circuit model.

*Case 2:* For more practical situations, $L_L \neq 0$, $R_S \neq 0$, Eq. (6) is solved through a tedious algebra process[9] to estimate the location of characteristic roots on the $P$-$Q$-$T$ three coordinates, and to obtain the stability and instability criteria. The stability and instability criteria can be reached by letting $P>0$, $Q>0$, and $T>0$, and letting $P<0$, respectively, and are given by Eqs. (11a) and (11b), respectively

$$\frac{|R_D|L_L}{L_Q} < R < \frac{L_L + L_Q}{|R_D|C}, \quad R > |R_D|, \tag{11a}$$

$$R < \frac{|R_D|L_L}{L_Q}. \tag{11b}$$

From Eq. (11b), whether the unstable oscillation will occur or not is only related to the inductive elements of $L_L$ and $L_Q$ and the NDC element $R_D$; there is no capacitance involved. Therefore, we may assume that the oscillation phenomenon appearing in the NDC region depends mainly on the inductance and is less influenced by the capacitance. In the practical case of measuring RTD $I$-$V$ characteristics, $R_L$ is presumably equal to zero (during $I$-$V$ curve measurement, looking into the measuring setup is usually high), and if $R = R_S = R_D$, then the stray inductance $L_L$ must be kept smaller than quantum well inductance $L_Q$ to prevent RTD from getting unstable oscillation.

### C. Model (c)

A proposed RTD model as shown in Fig. 4 (of which uncharacterized inductance and quantum well inductance are both part of the model components) is analyzed. The cubic characteristic equation and the values of $P$, $Q$, and $T$ for Fig. 4 are derived, and it has been found that they have the same forms as those of Eqs. (6) and (7), respectively. Assuming $R_S=0$ and $L_L=0$, and by letting $P>0$, $Q>0$, and $T>0$, for stable conditions, and letting $P<0$ for unstable conditions, we will have the same stability and instability criteria as Eqs. (11a) and (11b), respectively.

## III. NUMERICAL VERIFICATION

To verify the applicability of the derived stability and instability criteria, several published RTD structures[5,10–13] are adopted. The related parameters used in the calculation are based on the following descriptions.

It was shown that the large-signal inductance is approximated by $L=\tau_1 \ R_D$, and $\tau_1=\hbar/\Gamma_1$,[6] where $\tau_1$ is the electron lifetime of the first excited quasibound state in the quantum well, $R_D$ is the minimum magnitude in the NDC region, $\hbar$ is Planck's constant, and $\Gamma_1$ is the full width at half maximum of the first transmission probability function $T^*T$. The capacitance is difficult to measure and can be calculated from the numerical solution to Poisson's equation in the active region of the RTD. The quantum well inductance is calculated using $R_D=1/G_{\max}$, where $G_{\max}$ is the maximum of the negative differential conductance and can be obtained by differentiating the $I$-$V$ curve of RTD, which is simulated from the experimental $I$-$V$ data by using a new RTD modeling method.[14]

Referring to sample 1 in Refs. 10 and 6, the following parameters are calculated and used: $\tau_1=6$ pS, $C=77$ pF, and $G_{\max}=-30$ mS, and are estimated by the stability criteria of Eq. (10a)

$$|R_D| < R_L < \frac{L_Q}{|R_D|C} \Rightarrow 33\ \Omega < R_L < 78\ \Omega.$$

The expression for the above inequality is true, and it implies that a stable, continuous (no oscillation) NDC region is expected to exist in the $I$-$V$ curve of RTD as shown in the experimentally measured $I$-$V$ characteristics of Fig. 5. We were not able to use the instability criteria of Eq. (10b) to do the numerical verification for all the samples mentioned in this article, because the stray inductance $L_L$ is not available.

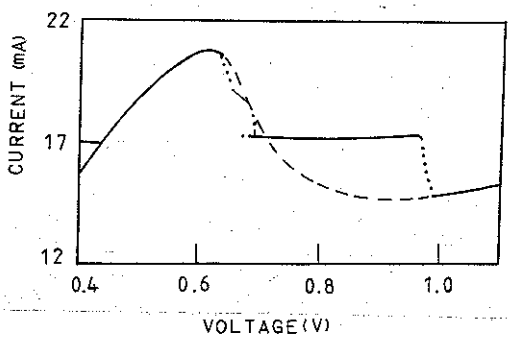


FIG. 6. Experimental $I$-$V$ characteristics (solid and dotted) and theoretical curve (dashed) of RTD sample 2 adopted from Brown *et al.*

However, to test if the $I$-$V$ curve of RTD has unstable oscillation in the NDC region, we can alternatively use the stability criteria.

Referring to sample 2 in Ref. 11, the following parameters are calculated and used: $\tau_1=0.11$ pS, $C=18.5$ pF, and $G_{\max}=-58$ mS, and are estimated by the stability criteria of Eq. (10a),

$$|R_D|<R_L<\frac{L_Q}{|R_D|C}\Rightarrow 17\ \Omega<R_L<5.9\ \Omega.$$

The expression for the above inequality is trivial. Therefore, a stable NDC region does not exist in the $I$-$V$ curve but an unstable oscillation phenomenon (discontinuous curve) appears instead, and this can be verified by Fig. 6.

Referring to sample 3 in Ref. 12, the following parameters are calculated and used: $\tau_1=90$ pS, $C=28$ pF, and $G_{\max}=-20$ mS, and are estimated by the stability criteria of Eq. (10a),

$$|R_D|<R_L<\frac{L_Q}{|R_D|C}\Rightarrow 50\ \Omega<R_L<32\ \Omega.$$

The above inequality is trivial from the numerical verification, so a stable NDC region will not exist but a discontinuous, unstable oscillation phenomenon occurs, as shown in Fig. 7.

Referring to sample 4 in Ref. 13, the following parameters are calculated and used: $\tau_1=2.64$ pS, $C=19$ pF, and $G_{\max}=-26$ mS, and are tested by the stability criteria of Eq. (10a),

$$|R_D|<R_L<\frac{L_Q}{|R_D|C}\Rightarrow 38.5\ \Omega<R_L<13.9\ \Omega.$$

The above inequality is trivial, so a stable NDC region cannot exist but an unstable oscillation phenomenon is shown instead, as illustrated in Fig. 8.

Referring to structure A of sample 5 in Ref. 5, the following parameters are calculated and used: $L=1.01$ nH, $C=3$ pF, and $G_{\max}=-500$ mS, and are tested by the stability criteria of Eq. (3a),

$$\frac{L}{|R_D|C}<R<|R_D|\Rightarrow 168\ \Omega<R<2\ \Omega.$$

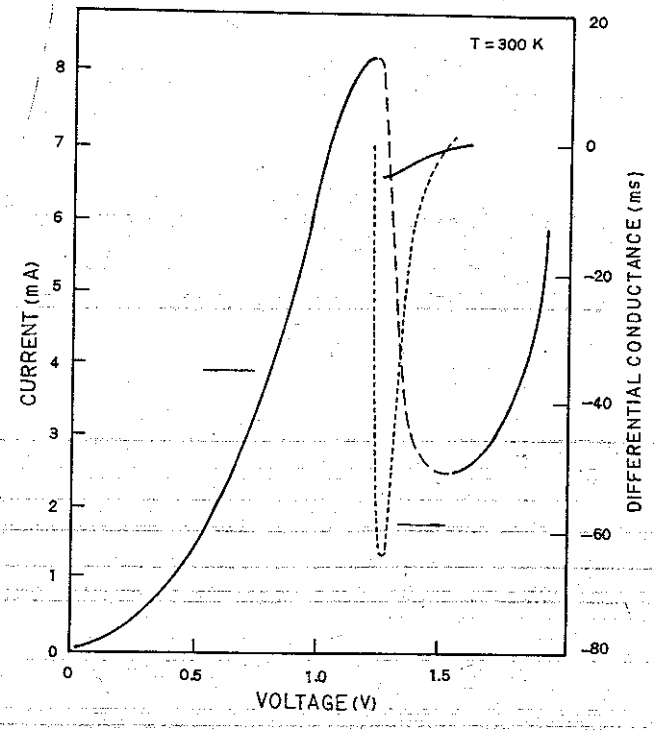


FIG. 7. Experimental $I$-$V$ characteristics (solid) and theoretical curve (dashed) of RTD sample 3 adopted from Brown *et al.*

The above inequality is trivial, so we have an unstable oscillation phenomenon appearing in Fig. 9(a).

Referring to structure B of sample 5 in Ref. 5, the following parameters are calculated and used: $L=0.93$ nH, $C=2.75$ pF, and $G_{\max}=-175$ mS, and are tested by the stability criteria of Eq. (3a)

$$\frac{L}{|R_D|C}<R<|R_D|\Rightarrow 59\ \Omega<R<5.7\ \Omega.$$

The above inequality is trivial in the numerical verification, so again an unstable oscillation phenomenon comes out in Fig. 9(a).

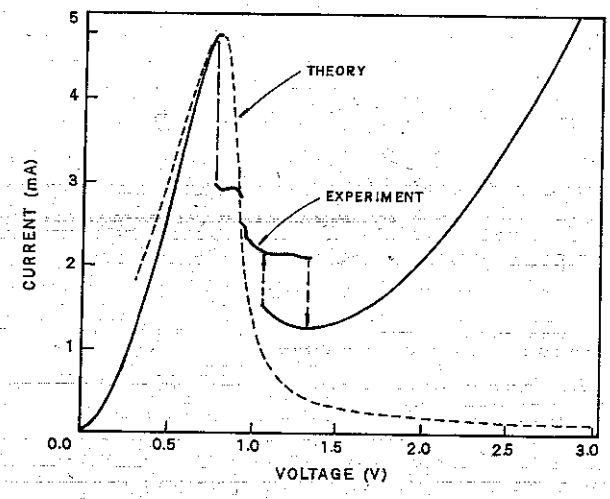


FIG. 8. Experimental $I$-$V$ characteristics (solid) and theoretical curve (dashed) of RTD sample 4 adopted from Brown *et al.*

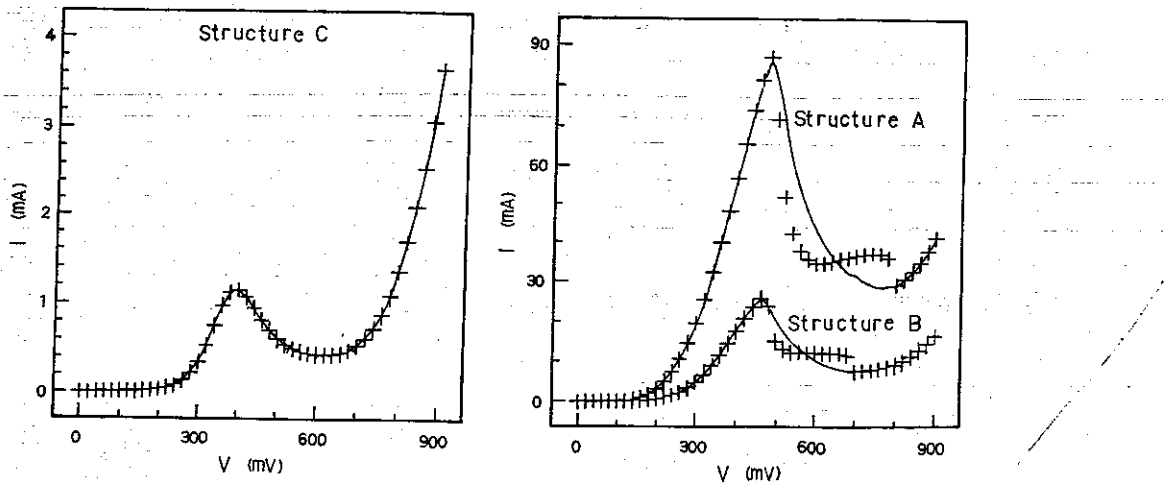


FIG. 9. Typical measured $I$-$V$ characteristics for the RTD three structures from Gering *et al.*, the plus symbols indicate the data points while the solid line is the nonoscillating $I$-$V$ curve. (a) Structures A and B show the unstable oscillation phenomenon in the NDR region. (b) Structure C shows the stable $I$-$V$ characteristics.

Referring to structure C of sample 5 in Ref. 5, the following parameters are calculated and used: $L=0.89$ nH, $C=2.6$ pF, and $G_{max}=-6.43$ mS, and are tested by the stability criteria of Eq. (3a),

$$\frac{L}{|R_D|C}<R<|R_D|\Rightarrow 2.2\ \Omega<R<1.55.5\ \Omega.$$

The above inequality is true for the expression, and we do have a continuous, stable (no oscillation) NDC region in the $I$-$V$ curve as shown in Fig. 9(b).

From the above numerical verification for all the RTD samples we mentioned, the derived stability criteria are valid to predict the occurrence of the unstable oscillation in the NDC region of the $I$-$V$ curve of RTD.

## IV. SIMULATION

To collaborate the efficacy of the derived stability and instability criteria with the measured experimental $I$-$V$ characteristics, we perform the $I$-$V$ curve simulation. An RTD structure[10] was considered for the SPICE simulation to show that the unstable oscillation phenomenon appears in the NDC region based on the derived stability or instability criteria. From our previous work,[14,15] we were able to obtain the continuous and stable NDC region of the dc $I$-$V$ curve tracing using an existing new modeling method. Extending our previously reported SPICE simulation result for the stable $I$-$V$ curve of RTD, the SPICE simulations of the discontinuous, unstable oscillation in the NDC region of RTD are carried out by varying the value of the RTD series resistance $R_S$ for the new RTD modeling method. The reason for that is it has shown that the derived stability and instability criteria are only relevant to three elements of $R_D$, $L$, and $C$, and the new modeling method mainly depends on the element $R_S$. If we change the value of $R_S$ in the simulation, the threshold (balance) point between the stable condition and the unstable condition will be reached at a certain value of $R_S$, which will also meet the requirement of the stability or instability criteria and the unstable oscillation phenomenon shows up in the NDC region. [In the simulation, $R_S$ represents the sum of the parasitic load resistance in $I$-$V$ characteristics measurement and the intrinsic series resistance of RTD as shown in Figs. 1, 3, and 4 and it is equivalent to $|R_D|$ of Eqs. (3) and (11).] We use the new RTD modeling method to perform SPICE simulation to the sample in Ref. 10 with the intrinsic series resistance of $R_S=5\ \Omega$. This value of $R_S$ was measured and corresponds to the small-signal terminal impedance.[6] The simulated dc $I$-$V$ characteristics with a stable NDC region was observed as shown in Fig. 10 (Figs. 3–8) and the NDC region remains stable if $R_S$ values varying in the small range. As $R_S$ increases to a certain threshold value, a flattened and broken section resulting in the discontinuity in the NDC region will gradually occur. Figure 11 shows the SPICE simulation plot appearing as the widest flattened line in the NDC region with the value of $R_S=35\ \Omega$. The value of $L/C$ in Eqs. (3) and (11), which indicates the degree of nonlinearity (extent of flatness), is assumed to be very large [$C$ is very small, 77 (ff)] which causes the apparent change of the wave form. For further increasing $R_S$, the magnitude of the flattened line between two positive slope segments (between a

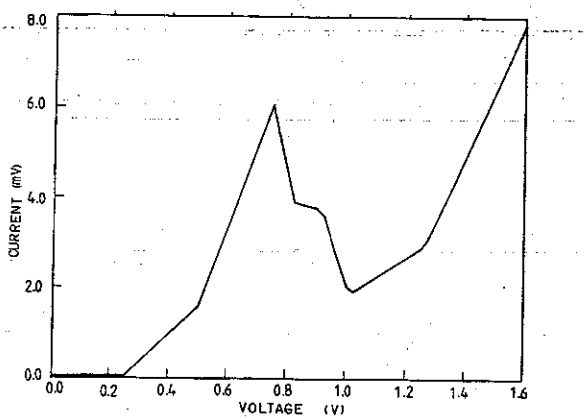


FIG. 10. Simulated $I$-$V$ characteristics from Huang *et al.*'s RTD sample using a new RTD modeling method.

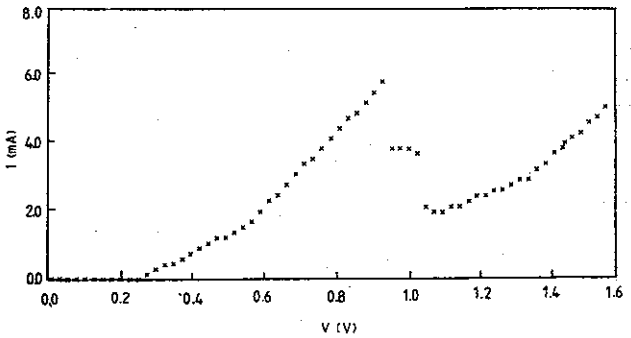


FIG. 11. Simulated $I$-$V$ characteristics result of the predicted flattened section in the NDC region from Huang *et al.*'s RTD sample using a new RTD modeling method.

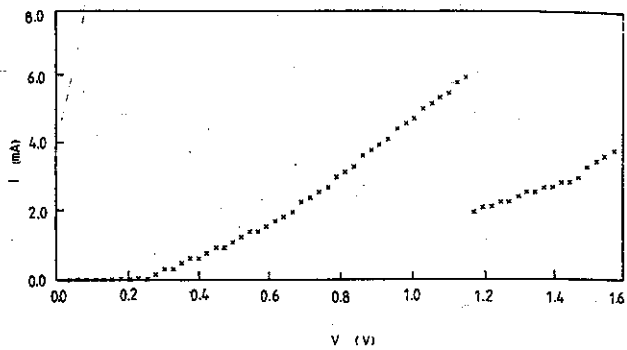


FIG. 12. Simulated $I$-$V$ characteristics result of the predicted broken section in the NDC region from Huang *et al.*'s RTD sample using a new RTD modeling method.

peak point and valley point) is reduced, and the slope of the first positive slope segment is decreasing. Accidentally, this slope shift in the $I$-$V$ curve which is caused by the increase of $R_S$ is consistent with the effect of the extra addition in spacer layers of RTD.[16] The broken section in the NDC region of this RTD sample eventually occurs as the width of the flattened line keeps narrowing. When the value of $R_S$ reaches 50 Ω, Fig. 12 shows, clearly, the separation (blank) between a peak point and valley point with no flattened section appearing in the NDC region.

## V. CONCLUSIONS

The theoretical derivation of the stability and instability criteria in the $I$-$V$ characteristics of RTD by using circuit theory analysis is discussed in detail. In order to verify the applicability of the derived formula, we have performed a numerical verification to the derived formula using several published RTD structures as samples, and it shows good agreement with the correct predictions between the derived results and the experimentally measured stable or unstable NDC region of $I$-$V$ characteristics. By using a new RTD modeling method we have also presented a SPICE simulation based on experimental stable $I$-$V$ data to show how the discontinuous, unstable oscillation phenomenon will occur if the parameters of an RTD device meet the requirement of the derived stability or instability criteria. From the derived formulas, it is known that to prevent the appearance of discontinuity, unstable oscillation (either with the flattened or broken section) within the NDC region, care must be taken for the intrinsic series resistance or parasitic load resistance, which will exist in designing the RTD structure or particular in measuring the $I$-$V$ curve and in turn impact the performance of RTD oscillators.

[1] T. J. Shewchuck, J. M. Gering, P. C. Chapin, P. D. Coleman, W. Kopp, C. K. Peng, and H. Morkoc, Appl. Phys. Lett. **47**, 986 (1985).
[2] J. F. Young, B. M. Wood, H. C. Liu, M. Buchanen, D. Landheer, A. J. SpringThorpe, and P. Mandeville, Appl. Phys. Lett. **52**, 1398 (1988).
[3] C. Y. Belhadj, K. P. Martin, S. Ben Amor, J. J. L. Rascol, R. J. Higgins, R. C. Potter, H. Hier, and E. Hempfling, Appl. Phys. Lett. **57**, 58 (1990).
[4] E. S. Heliman, K. L. Lear, and J. S. Harris, Jr., J. Appl. Phys. **64**, 2798 (1988).
[5] J. M. Gering, D. A. Crim, D. G. Morgan, P. D. Coleman, W. Kopp, and H. Morkoc, J. Appl. Phys. **61**, 271 (1987).
[6] E. R. Brown, C. D. Parker, and T. C. L. G. Sollner, Appl. Phys. Lett. **54**, 934 (1989).
[7] W. J. Cunningham, *Introduction to Nonlinear Analysis* (McGraw Hill, New York, 1958), pp. 84–120.
[8] W. C. G. Ortel, Proc. IEEE **54**, 936 (1966).
[9] N. Jacobson, *Basic Algebra I* (W. H. Freeman & Co., New York, 1910), pp. 211–264.
[10] C. I. Huang, M. J. Paulus, C. A. Bozada, S. C. Dudley, K. R. Evans, C. E. Stutz, R. L. Jones, and M. E. Cheney, Appl. Phys. Lett. **51**, 121 (1987).
[11] E. R. Brown, T. C. L. G. Sollner, C. D. Parker, W. D. Goodhue, and C. L. Chen, Appl. Phys. Lett. **55**, 1777 (1989).
[12] E. R. Brown, J. R. Söderstrom, C. D. Parker, L. J. Mahoney, K. M. Molvar, and T. C. McGill, Appl. Phys. Lett. **58**, 2291 (1991).
[13] E. R. Brown, W. D. Goodhue, and T. C. L. G. Sollner, J. Appl. Phys. **64**, 1519 (1988).
[14] C. Y. Huang, J. E. Morris, Y. K. Su, and T. H. Kuo, Electron. Lett. **30**, 1012 (1994).
[15] C. Y. Huang, J. E. Morris, and Y. K. Su, IEEE Trans. Electron Devices **42**, 1705 (1995).
[16] T. Wei, and S. Stapleton, J. Appl. Phys. **76**, 1287 (1994).